Towards equilibration and thermalization between finite quantum systems: Unitary emulation of dephasing effects and inelastic interactions

Manas Kulkarni,[1,2] Kunal L. Tiwari,[1,2] and Dvira Segal[1]

[1]*Chemical Physics Theory Group, Department of Chemistry, University of Toronto, 80 Saint George St. Toronto, Ontario M5S 3H6, Canada*

[2]*Department of Physics, University of Toronto, 60 Saint George St. Toronto, Ontario M5S 1A7, Canada*

(Received 11 June 2012; published 12 October 2012)

Using a unitary time evolution scheme, we demonstrate an approach towards a Gibbs-like equilibrium state, with a common temperature and a chemical potential, of two metallic grains connected by a weak link prepared with a different number of noninteracting electrons. This unitary equilibration is achieved by coupling the link to a third finite mesoreservoir that can emulate dephasing and inelastic processes. The two quantum systems equilibrate but do not evolve towards a canonical state when mimicking dephasing effects only. Exact numerical results are supported by analytic calculations based on an extension of the quantum Langevin equation approach, providing the dynamics of the total density matrix.

DOI: 10.1103/PhysRevB.86.155424 PACS number(s): 05.30.−d, 03.65.Aa, 03.65.Yz, 72.10.−d

I. INTRODUCTION

How do quantum systems equilibrate from a certain nonequilibrium initial condition (e.g., a quench)?[1] Cold atoms in optical lattices have come to offer a clean experimental setup[2] that has sparked a renewed attention in this fundamental topic. One could address this question with (at least) three distinct setups: (i) study the evolution towards equilibrium of an isolated quantum system (e.g., in the time-averaged sense);[3,4] (ii) monitor the equilibration of a subsystem with a few degrees freedom (DOF) coupled to a thermal reservoir (e.g., in the small trace distance sense);[5,6] (iii) observe the process of mutual equilibration between two connected finite quantum systems.[7] Despite intense efforts, general results are still missing.[8–10]

In this work, we show that a finite and closed noninteracting quantum system, initialized to a nonequilibrium state, can evolve unitarily into an equilibrium state, before recurrence. Particularly, we consider two finite metallic quantum systems, L and R, connected through a weak link, a quantum dot. The link is further coupled to a third finite dissipationless and noninteracting Fermi sea, referred to as a probe.[11–13] Mutual equilibration in the L-dot-R system is reached by setting the initial distribution of the probe such that dephasing effects are emulated on the quantum dot. An approach to thermal equilibrium is demonstrated by initializing the probe electron distribution to effectively enact inelastic interactions on the dot. The total system, including the metal grains, dot, and probe, is finite and closed, thus its quantum dynamics can be followed exactly numerically. Simulations are augmented by an extension of the quantum Langevin equation (QLE) method to reveal reservoirs dynamics. Equilibration dynamics in the presence of inelastic scattering processes (e.g., electron-phonon coupling) is an extremely challenging problem.[15–18] Our present study demonstrates that unitary time evolution of a system that phenomenologically captures such interactions may yield an equilibrium (and even a thermal) state.

II. MODEL

We study the noninteracting Anderson model with a single electronic level (dot) coupled to two metallic grains $\nu = L, R$,[19] with identical densities of states and sharp cutoffs at $\pm D$. The grains do not couple directly, only through their weak hybridization with the dot (see Fig. 1). We refer to the metal grains, each comprised of $N \sim 100$ to 1000 electronic states and $n \sim 50$ to 500 electrons, as "reservoirs" to indicate that they have a high density of states that allows their effect on the dot electron to be absorbed into a positive real self-energy function. In turn, this allows for a QLE description.[20] The Hamiltonian takes the form

$$H_0 = H_L + H_R + H_W + V_L + V_R, \tag{1}$$

where $H_{L,R,W}$ represents the Hamiltonian for left reservoir, right reservoir, and dot, respectively. The term V_ν denotes the coupling of the dot to the ν reservoir,

$$\begin{aligned} H_L &= \sum_l \epsilon_l c_l^\dagger c_l, \quad H_R = \sum_r \epsilon_r c_r^\dagger c_r, \quad H_W = \epsilon_d c_d^\dagger c_d \\ V_L &= \sum_l v_l c_d^\dagger c_l + \text{H.c.} \quad V_R = \sum_r v_r c_d^\dagger c_r + \text{H.c.} \end{aligned} \tag{2}$$

Here, $c_k^\dagger$ (c_k) are fermionic creation (annihilation) operators of the left reservoir, $l \in L$, right reservoir, $r \in R$, or the dot (d). We assume that v_l and v_r are real numbers, and define the hybridization as $\Gamma_\nu(\epsilon) = \pi \sum_{k\in\nu} v_k^2 \delta(\epsilon - \epsilon_k)$, taken in practice to be energy independent. A factorized initial state is assumed, with the dot empty and the reservoirs prepared in a distinct diagonal state at a chemical potential $\mu_L \neq \mu_R$ and inverse temperature $\beta = 1/T$, satisfying the distribution $f_\nu(\epsilon) = [e^{\beta(\epsilon-\mu_\nu)} + 1]^{-1}$.

At t_0 the reservoirs are put into contact through the dot, and their dynamics is followed using either an exact scheme or a QLE approach (details below). The resulting populations dynamics, $p(\epsilon_k) \equiv \langle c_k^\dagger c_k \rangle$, are depicted in Fig. 2(a) with a near perfect agreement of the two methods. When the dot level is placed within the bias window, a resonance feature forms at about ϵ_d. This dynamics is reversible, with a characteristic time $\tau_d \sim 2\pi/\Delta E$; $\Delta E = 2D/N$ is the mean spacing between energy levels.[8] At this time, a depletion of certain reservoir states occurs, and the dot dynamics begins to reverse.

Elastic dephasing or inelastic scattering processes on the dot can be emulated with a probe. The Hamiltonian (2) is

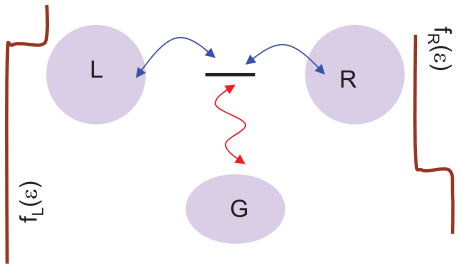

FIG. 1. (Color online) Two metallic grains, L and R, are separately prepared in a grand canonical diagonal state; the initial population is plotted at the boundaries. At t_0 these reservoirs are put into contact through a single electronic state. The G reservoir (probe) emulates decohering and inelastic effects.

augmented with an additional (finite size and dissipationless) electron reservoir G,

$$H = H_0 + H_G + V_G, \tag{3}$$

where $H_G = \sum_g \epsilon_g c_g^\dagger c_g$ and $V_G = \sum_g v_g c_g^\dagger c_d + \text{H.c.}$ We define $\Gamma_G(\epsilon) = \pi \sum_{k\in G} v_k^2 \delta(\epsilon - \epsilon_k)$, and henceforth assume it to be a constant. In the case of the voltage probe,[11,12] emulating inelastic effects, we demand that the net charge current from the dot to the G unit vanishes, $i_G = 0$. Implementation of the dephasing probe, fabricating elastic decoherence, necessitates

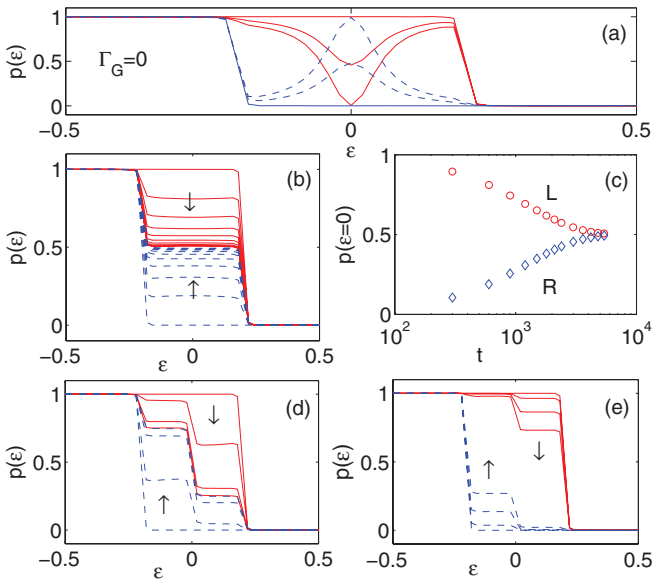

FIG. 2. (Color online) Dynamics under a unitary evolution, Eq. (4). (a) Population of the L (full) and R (dashed) reservoirs, $\Gamma_G = 0$. We show results at $t = 0$, 180, 340 as the resonance pattern develops in time. (b)–(c) Equilibration with a dephasing probe, $\Gamma_G = 0.4$, approaching a noncanonical equilibrium state. The L (full) and R (dashed) populations are shown at $t = 0, \delta t, \ldots, 9\delta t$, $\delta t = 600$. (d) Approaching thermal equilibrium with a voltage probe, $\Gamma_G = 0.4$ with the L (full) and R (dashed) populations shown at $t = 0, 600, 2500, 6000$. (e) Same as (d) with $\Gamma_G = 5$. In all panels $\beta = 200$, $\Gamma_L = \Gamma_R = 0.025$, $\epsilon_d = 0$, $\mu_L = -\mu_R = 0.2$, $D = 1$, $N_{L,R} = 100$, and $N_G = 2000$ electronic states in each reservoir. The arrows mark the direction of propagation in time.

the stronger requirement $i_G(\epsilon) = 0$ (i.e., the charge current at a given energy should vanish). It should be emphasized that conventional usage of the probe terminology refers to an open system scenario.[11–14] In contrast, in the present modeling the G reservoir is a finite-closed quantum system, only initialized with a certain special distribution to provide phase loss and possibly energy reorganization for electrons, acting like a conventional probe. After its preparation, the G unit, with other parts of the system, is left undisturbed. This allows us to time evolve the total density matrix under H_0 or H in a unitary way, as we explain next.

III. METHODS

A. Exact results with trace formula

Using a unitary, brute force calculation, we numerically evolve the expectation value of $A \equiv c_j^\dagger c_k$,

$$\begin{aligned}\langle A(t)\rangle &= \text{Tr}[\rho(t_0) e^{iHt} A e^{-iHt}] \\ &= \lim_{\lambda\to 0} \frac{\partial}{\partial\lambda} \text{Tr}[\rho_L \rho_R \rho_G \rho_d e^{iHt} e^{\lambda A} e^{-iHt}],\end{aligned} \tag{4}$$

using the fermionic trace formula.[21,22] Here, $\rho_\nu = e^{-\beta(H_\nu - \mu_\nu N_\nu)}/Z_\nu$, Z_ν is the partition function, $\nu = L, R, G$. ρ_d stands for the dot initial density matrix, and we trace over all DOF. To include inelastic scattering effects of electrons on the dot, we implement a voltage probe initializing the probe population to $f_G(\epsilon) = [e^{\beta(\epsilon-\mu_G)} + 1]^{-1}$. The chemical potential μ_G is taken such that $i_G \equiv \frac{d}{dt}\sum_g \langle c_g^\dagger c_g\rangle = 0$ is satisfied. With the motivation to explore behavior beyond the linear response regime,[23] we retrieve μ_G numerically, by employing the Newton-Raphson method.[24] Practically, as the reservoirs are dense, to a very good approximation the energy resolved charge current into G can be written as

$$i_G(\epsilon) = \frac{2\Gamma_G}{\pi} \frac{\Gamma_R[f_G(\epsilon) - f_R(\epsilon)] + \Gamma_L[f_G(\epsilon) - f_L(\epsilon)]}{(\epsilon - \epsilon_d)^2 + \Gamma^2} \tag{5}$$

in the quasi-steady-state (QSS) limit, with the total current $i_G = \int i_G(\epsilon) d\epsilon$. Here $\Gamma = \Gamma_L + \Gamma_R + \Gamma_G$. Quasi-elastic scattering effects are implemented within a dephasing probe, by demanding that $i_G(\epsilon) = 0$, to yield $f_G(\epsilon) = \frac{\Gamma_R f_R(\epsilon) + \Gamma_L f_L(\epsilon)}{\Gamma_R + \Gamma_L}$. In principle, one should adjust the probe throughout the simulation to eliminate leakage from the L-dot-R system. However, we found that the probe condition was well satisfied in all simulation times, once set according to the QSS condition.

Results from this exact-unitary scheme, up to the recurrence time $\tau_{\text{rec}} \propto \sum_{i=L,R,G} N_i$, are displayed in Figs. 2(b)–2(e) and are discussed below. The system approaches equilibrium (both probes), and even thermal equilibrium (voltage probe).

B. Quantum Langevin equation

The quantum Langevin equation method, originally developed for describing subsystem dynamics only,[20,23,25,26] is extended here to capture the exact reservoirs dynamics up to a certain time. We explain the steps involved to highlight the underling approximations and set limits for the method applicability. We outline the derivation in the absence of

the probe, generalized later to include such a device. In the Heisenberg representation the l operators follow

$$c_l(t) = e^{-i\epsilon_l(t-t_0)}c_l(t_0) - iv_l\int_{t_0}^{t} d\tau e^{-i\epsilon_l(t-\tau)}c_d(\tau)d\tau. \quad (6)$$

Similar relations hold for the r operators. We substitute these expressions into the dot equation of motion (EOM),

$$\dot{c}_d = -i\epsilon_d c_d - i\sum_l v_l c_l - i\sum_r v_r c_r, \quad (7)$$

to find the exact result:

$$\dot{c}_d = -i\epsilon_d c_d - \int_{t_0}^{t} d\tau \sum_l v_l^2 e^{-i\epsilon_l(t-\tau)}c_d(\tau) - \int_{t_0}^{t} d\tau \sum_r v_r^2 e^{-i\epsilon_r(t-\tau)}c_d(\tau) - i\eta^L(t) - i\eta^R(t). \quad (8)$$

Here, $\eta^L(t) \equiv \sum_l v_l e^{-i\epsilon_l(t-t_0)}c_l(t_0)$, and similarly η^R, represent "noise." We assume that the second and third terms each reduce into decay terms, further inducing an energy shift of the dot energy, absorbed into the definition of ϵ_d. This is justified as the metal grains play the role of charge and energy reservoirs for the dot. Under the Markovian approximation, we reach the (time local) QLE

$$\dot{c}_d = -i\epsilon_d c_d - i\eta^L(t) - i\eta^R(t) - \Gamma(\epsilon_d)c_d, \quad (9)$$

with $\Gamma(\epsilon) = \sum_{v=L,R}\Gamma_v(\epsilon)$ [e.g., $\Gamma_L(\epsilon) = \pi\sum_l v_l^2\delta(\epsilon-\epsilon_l)$]. We now use the exact equation (6) and the reduced result (9) to derive analytic expressions for the expectation values $\langle c_k^\dagger(t)c_j(t)\rangle \equiv \mathrm{Tr}[\rho(t_0)c_k^\dagger(t)c_j(t)]$; $k,j = l,r,d$, where $\rho(t_0) = \rho_d\otimes\rho_L\otimes\rho_R$ is the time-zero density matrix. The assumed initial condition is

$$\begin{aligned}\langle c_d^\dagger(t_0)c_d(t_0)\rangle &= 0,\\ \langle c_l^\dagger(t_0)c_l(t_0)\rangle &= f_L(\epsilon_l)\equiv f_l,\\ \langle c_r^\dagger(t_0)c_r(t_0)\rangle &= f_R(\epsilon_r)\equiv f_r.\end{aligned} \quad (10)$$

The resolved occupations of the (e.g., L reservoir states) are given by three contributions

$$\begin{aligned}p(\epsilon_l) \equiv \langle c_l^\dagger(t)c_l(t)\rangle &= \langle c_l^\dagger(t_0)c_l(t_0)\rangle\\ &+ iv_l e^{-i\epsilon_l(t-t_0)}\int_{t_0}^{t} e^{i\epsilon_l(t-\tau)}\langle c_d^\dagger(\tau)c_l(t_0)\rangle d\tau + \text{c.c.}\\ &+ v_l^2\int_{t_0}^{t}\int_{t_0}^{t} d\tau_1 d\tau_2\langle c_d^\dagger(\tau_1)c_d(\tau_2)\rangle e^{i\epsilon_l(t-\tau_1)}e^{-i\epsilon_l(t-\tau_2)}.\end{aligned}$$

The first term accommodates the initial condition. The second (F_2) and third (F_3) contributions are given by

$$F_2 = -v_l^2 f_l\times(t-t_0)\frac{2\Gamma}{\Gamma^2+\epsilon_{dl}^2} - 2v_l^2 f_l\frac{\epsilon_{dl}^2-\Gamma^2}{\left[\epsilon_{dl}^2+\Gamma^2\right]^2} + \frac{v_l^2 f_l e^{-\Gamma(t-t_0)}}{\left[\epsilon_{dl}^2+\Gamma^2\right]^2}\left\{2\left[\epsilon_{dl}^2-\Gamma^2\right]\cos[\epsilon_{dl}(t-t_0)] + 4\epsilon_{dl}\Gamma\sin[\epsilon_{dl}(t-t_0)]\right\}$$

$$F_3 = v_l{}^2\sum_{k'\in L,R}\frac{v_{k'}{}^2 f_{k'}}{\Gamma^2+\epsilon_{dk'}^2}\left\{\frac{4\sin^2\left[\frac{\epsilon_{lk'}}{2}(t-t_0)\right]}{\epsilon_{lk'}^2} + \frac{1}{\Gamma^2+\epsilon_{dl}^2}[e^{-2\Gamma(t-t_0)}+1-e^{(t-t_0)(i\epsilon_{dl}-\Gamma)}-e^{-(t-t_0)(i\epsilon_{dl}+\Gamma)}] + \left[\frac{1-e^{-(t-t_0)(\Gamma+i\epsilon_{dl})}+e^{-(t-t_0)(\Gamma+i\epsilon_{dk'})}-e^{-i(t-t_0)\epsilon_{lk'}}}{(\epsilon_{dl}-i\Gamma)\epsilon_{lk'}}+\text{c.c.}\right]\right\}, \quad (11)$$

with $\epsilon_{jk} = \epsilon_j - \epsilon_k$ and $\Gamma \equiv \Gamma(\epsilon_d)$. We have similarly derived closed expressions for *all* density matrix elements [e.g., $\langle c_l^\dagger(t)c_{l'}(t)\rangle$] ($l \neq l'$). Since the reservoirs are large, after a short time, $\tau_t \gtrsim 2/\Gamma$, the dot occupation remains fixed at a QSS value.

In the presence of the probe, the expression $p(\epsilon_l)$, and other expectation values, stay formally intact; one needs to (i) redefine the total hybridization, $\Gamma = \Gamma_L + \Gamma_R + \Gamma_G$, (ii) augment the summation in F_3 by $k' \in G$ terms, and (iii) set the G reservoir initial distribution to satisfy the probe condition. Equation (11) extends the standard QLE description to reveal the dynamics of the reservoirs DOF. With the probe, it captures a nontrivial evolution towards an equilibrium state. While the QLE is not a unitary scheme [Eq. (9) describes an irreversible behavior for the dot], it excellently reproduces the exact dynamics up to $\tau_d \sim \pi N/D$ where (partial) recurrence behavior begins to display itself.[8]

IV. RESULTS

We define thermal equilibration in our study by adjusting the conditions of Refs. 5 and 10 to demand that (i) the system should equilibrate (i.e., evolve towards a particular state) and stay close to it for almost all time. The equilibrium state should be (ii) independent of the dot properties and initial state, (iii) insensitive to the precise initial state of the L and R reservoirs, (iv) close to diagonal in the energy basis of its eigen-Hamiltonian, and (v) a canonical state.

We use the exact unitary method and follow the reservoirs' mutual equilibration process up to τ_{rec}, the time when recurrence features start to show, using either a dephasing probe or a voltage probe [see Figs. 2(b)–2(e)]. A clear evolution towards an equilibrium state is demonstrated in both cases. With a dephasing probe [Figs. 2(b)–2(c)], the populations of the two reservoirs relax to a two-step function with $p(\mu_R < \epsilon < \mu_L) \sim 0.5$. Because electrons from L lose their phase memory on the dot, half of them populate the R side on average in the long time limit. This equilibrium state is sensitive to the precise details of the initial electron distribution, as energy redistribution is not allowed. We build a large G to delay recurrence, but results at earlier times do not depend on the size of G, reinforcing the observation that G acts as an agent in driving the L-R mutual equilibration. When inelastic effects are mimicked with a voltage probe and Γ_G is large enough

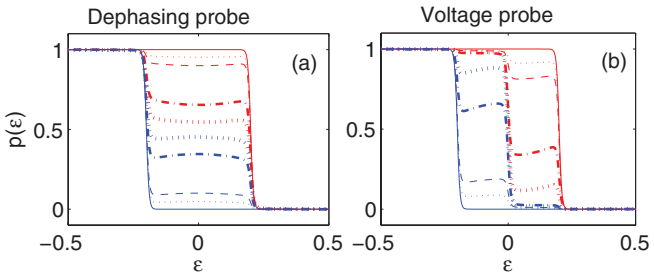

FIG. 3. (Color online) QLE results. (a) Approaching a noncanonical equilibrium state with a dephasing probe, L-reservoir (five top lines) and R-reservoir (five bottom lines) occupation functions. (b) Approaching thermal equilibrium with a voltage probe, L (five rightmost lines) and R (five leftmost lines) occupation functions. $\Gamma_G = 0.4$ and $t = 0$ (full), $t = 750$ (dotted), $t = 1500$ (dashed), $t = 7500$ (dashed-dotted), and $t = 15 \times 10^3$ (heavy dotted). The last two lines were generated by restarting the QLE dynamics when approaching $t = m\tau_d$, m is an integer. Parameters are the same as in Fig. 2, besides $N_{L,R,G} = 500$.

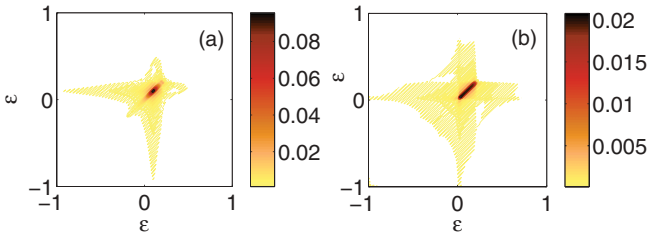

FIG. 4. (Color online) Absolute values of the density matrix elements $\rho_{l,l'}$ at $t = 1500$ (a) $\Gamma_G = 0$, (b) using a voltage probe, $\Gamma_G = 0.4$. Other parameters are the same as in Fig. 3(b), $\epsilon_d = 0.1$.

[Fig. 2(e)] the system does approach a Gibbs-like thermal state—a step function at zero temperature. Results are shown up to the recurrence time $\tau_{\rm rec}$, which emerges here before full thermalization takes place. At smaller Γ_G, a noncanonical equilibrium distribution develops [Fig. 2(d)] reflecting the contribution of coherent and (effectively) incoherent electrons in the dynamics.

Figure 3 displays results from the QLE method up to τ_d, where the technique breaks down. Numerically, the method failure is reflected by reservoirs' states occupation exceeding unity. Data at later times has been generated by restarting the simulation immediately before τ_d with initial conditions defined by the resultant L and R diagonal distributions and with the G reservoir readjusted to respect the probe condition. This process can be repeated, to reach a complete equilibration. Experimental realization is possible through fine adjustment of the probe,[14] which destroys coherences in the reservoirs at the prescribed time. We have also verified that while at $\Gamma_G = 0$ the resonance peak emerges around the energy ϵ_d, at nonzero Γ_G the buildup of the equilibrium state systematically occurs around the equilibrium Fermi energy. This holds even when the dot energy is placed *outside* the bias window.

Figure 4 displays the density matrix (DM) $\rho_{l,l'} = \langle c_l^\dagger c_{l'} \rangle$, excluding diagonals, with and without a voltage probe, produced by the QLE technique. This quantity is expected to oscillate in the long time limit since the Hamiltonian is not diagonal in the (local) l basis. We show results in this basis, so as to manifest local ν-reservoir properties. A subtle complication is the fact that off-diagonal elements decay here (after the initial rise), even without a probe, as a result of the finite-bias assumed as an initial condition. There are three significant differences in the behavior of off-diagonal elements with and without the probe: (i) absolute values of the coherences, at any given time, are smaller for $\Gamma_G \neq 0$; (ii) the DM approaches a diagonal form (strict diagonal values are not shown) under the influence of the probe; (iii) oscillations occur around ϵ_d when $\Gamma_G = 0$. With the probe, contributions shift towards the equilibrium Fermi energy.

V. SUMMARY

We have provided evidence that finite closed quantum systems, evolving unitarily, can equilibrate and even thermalize by emulating phase memory loss and energy exchange processes for electrons on the link between these objects. Our results are significant for several reasons: (i) unitary evolution, emulating dephasing and inelastic scattering effects on a small, yet essential, subset of the total system can drive the system towards a global equilibrium state; (ii) we have not assumed the colloquial, restrictive, "nondegenerate energy gap" condition[3–5,7] in our study; (iii) we frame a tool, based on the QLE treatment,[20] for studying the dynamics of a large system composed of many DOF, by identifying a subsystem, resolving its dynamics, then using this information backward, exploring the evolution of the total DM. It is of interest to study energy-resolved dynamics in interacting electron systems, for elucidating the role of electron-electron interaction effects in the transport process.[27]

ACKNOWLEDGMENTS

This work has been supported by an NSERC discovery grant. M.K. thanks Diptiman Sen for useful discussions.

[1] A. Polkovnikov, K. Sengupta, A. Silva, and M. Vengalattore, Rev. Mod. Phys. **83**, 863 (2011).
[2] I. Bloch, J. Dalibard, and W. Zwerger, Rev. Mod. Phys. **80**, 885 (2008).
[3] P. Reimann, Phys. Rev. Lett. **101**, 190403 (2008); New J. Phys. **12**, 055027 (2010).
[4] A. J. Short, New J. Phys. **13**, 053009 (2011).
[5] N. Linden, S. Popescu, A. J. Short, and A. Winter, Phys. Rev. E **79**, 061103 (2009).
[6] J. Dajka, J. Luczka, and P. Hänggi, Phys. Rev. A **84**, 032120 (2011).
[7] A. V. Ponomarev, S. Denisov, and P. Hänggi, Phys. Rev. Lett. **106**, 010405 (2011).
[8] V. I. Yukalov, Laser Phys. Lett. **8**, 485 (2011).

[9]J.-S. Caux, and J. Mossel, J. Stat. Mech.: Theory Exp. (2011) P02023.
[10]C. Gogolin, M. P. Müller, and J. Eisert, Phys. Rev. Lett. **106**, 040401 (2011).
[11]M. Büttiker, Phys. Rev. B **32**, 1846 (1985); **33**, 3020 (1986).
[12]M. J. M. de Jong and C. W. J. Beenakker, Physica A **230**, 219 (1996).
[13]H. Forster, P. Samuelsson, S. Pilgram, and M. Buttiker, Phys. Rev. B **75**, 035340 (2007).
[14]P. Roulleau, F. Portier, P. Roche, A. Cavanna, G. Faini, U. Gennser, and D. Mailly, Phys. Rev. Lett. **102**, 236802 (2009).
[15]L. Mühlbacher and E. Rabani, Phys. Rev. Lett. **100**, 176403 (2008).
[16]H. Wang, I. Pshenichnyuk, R. Härtle, and M. Thoss, J. Chem. Phys. **135**, 244506 (2011).
[17]R. Hützen, S. Weiss, M. Thorwart, and R. Egger, Phys. Rev. B **85**, 121408 (2012).
[18]Y. Vinkler, A. Schiller, and N. Andrei, Phys. Rev. B **85**, 035411 (2012).
[19]P. W. Anderson, Phys. Rev. **124**, 41 (1961).
[20]G. W. Ford, J. T. Lewis, and R. F. O'Connell, Phys. Rev. A **37**, 4419 (1988).
[21]I. Klich, in *Quantum Noise in Mesoscopic Systems*, edited by Yu. V. Nazarov and Ya. M. Blanter (Kluwer, The Netherlands, 2003).
[22]D. Segal, A. J. Millis, and D. R. Reichman, Phys. Rev. B **82**, 205323 (2010); Phys. Chem. Chem. Phys. **13**, 14378 (2011).
[23]D. Roy and A. Dhar, Phys. Rev. B **75**, 195110 (2007).
[24]W. H. Press, B. P. Flannery, S. A. Teukosky, and W. T. Vetterling, *Numerical Recipes in C: The Art of Scientific Computing* (Cambridge University Press, Cambridge, 1992).
[25]A. Dhar and D. Sen, Phys. Rev. B **73**, 085119 (2006).
[26]A. Dhar, K. Saito, and P. Hänggi, Phys. Rev. E **85**, 011126 (2012).
[27]M. Kulkarni, K. L. Tiwari, and D. Segal, arXiv:1208.5725.